5-2011

Basins of Attraction in Stage Structured Populations

Georgia Waite Pfeiffer
College of William and Mary

Basins of Attraction in Stage Structured Populations

A thesis submitted in partial fulfillment of the requirement
for the degree of Bachelor of Science in Mathematics from
The College of William and Mary

by

Georgia Waite Pfeiffer

Accepted for Honors

Sarah Day, advisor

Junping Shi

Larry Leemis

Matthias Leu

Williamsburg, VA
April 22, 2011

Basins of Attraction in Stage Structured Populations

Georgia W. Pfeiffer

Undergraduate Honors Project

May 2011

Acknowledgements

Thank you to Dr. Sarah Day, Dr. Larry Leemis, and Dr. Junping Shi in the math department and Dr. Matthias Leu in the biology department for serving on the honors thesis examining committee. Particular thanks to Dr. Day for her work as my primary thesis advisor.

This project was started at Texas A&M as part of the summer Research Experience for Undergraduates under the supervision of Dr. May Boggess and Dr. Jay Walton in the math department with particular help from Dr. Masami Fujiwara in the department of wildlife and fisheries sciences.

Funding for the REU was jointly provided by the NSF (award number 0850470) and the Department of Defense. CSUMS funding was provided at William and Mary by the NSF

Abstract

The interaction between invasive and native species can be modeled through a Lefkovitch model using stage structured populations. In this study, we analyze population dynamics of a stage structured population, computing a basin of attraction around the non-trivial attracting equilibrium.This model can be naturally extended to include two or more species in which inter- and intra-specific competition is expressed through a density dependent fertility term. Preliminary results for the two species model will be discussed.

Contents

List of Figures

Chapter 1

Introduction

Ecosystems are built on a complex web of interactions between animals, plants and their environment. Species interactions just between animals can follow many diverse paths through cooperation and competition, often developing through co-evolution to create and refine interactions for the mutual benefit or defense against each other. In many cases, exotic or non-native species upset the established interactions and balance in ecosystems. Once exotic species establish themselves in a new environment, they are considered invasive. Human influence has brought about a much higher rate of non-native species introduction in ecosystems around the world, in many cases permanently establishing invasive species.

In many cases, these new introductions cause negative changes challenging the native species and lowering the value of the ecosystem. For example the introduction of avian malaria and mosquitos to Hawaii has severely damaged the native bird populations. Aggregating the effects of disease, human exploitation, habitat destruction, and direct interaction with introduced species, forty percent of native taxa have gone extinct [10]. Over half of the remaining taxa are considered endangered by federal standards. It is clear that the introduction of avian malaria has been a driving factor in this extinction because the remaining birds live at elevations uninhabitable by the mosquitos that spread the disease [10].

Not all invasive species bring about the destruction seen in native Hawaiian bird populations. Some non-native introductions have a more debatable role in their new environment. The North American red swamp crayfish, Procambarus clarkii, is a highly invasive species native to the southeastern United States and Mexico. It has spread nearly world-wide often changing ecosystems from clear-water habitats to turbid systems by feeding heavily on macrophytes, thereby allowing phytoplankton populations to dominate [17]. However, upon invading the Guadalquivir marshes in southwestern Spain, the crayfish became an important food source for several threatened avian species, sometimes making up over half of

their diet. The threatened bird populations increased significantly with the addition of red swamp crayfish [17]. The invasive crayfish did however have a negative impact on native crayfish populations and species at lower trophic levels.

The two examples above are meant to illustrate the complexity of invasive species dynamics as well as the growing prevalence of the issue. This paper is designed to develop the techniques needed to construct basins of attraction for neighborhoods of attracting equilibria, offering a more global picture to ecologists, who could then decide how a population needs to be controlled in order to reach a desired state. Basins of attraction will show us the collection of initial conditions that correspond to populations that will reach a specific neighborhood within a finite number of time steps. This would offer ecologists a larger "target region", where if the population could be forced to enter this region the dynamics of the of the system would then take over a lead to the desired result. The dynamics of each situation have to be evaluated as well as the repercussions of any kind of disturbance before biological control of invasive species is undertaken.

The model used in this paper can reflect a variety of relevant population interactions. For this study, it is primarily likened to invasive species dynamics. Within this context, the strength of this model lies in its applications to conservation efforts. Managing invasive species is a tremendous challenge to conservationists. We hope to show how mathematical analysis can be used on population models in a way that will allow conservationists to use resources more efficiently.

The first part of the paper details the population structure and life history strategies of hypothetical species and their interactions through competition for resources. We examine the stability of three types of equilibria, extinction, exclusion, and coexistence through linearization, answering questions about the system's behavior in a very small neighborhood surrounding the equilibria. Extinction, as the name suggests, refers to the trivial equilibrium where both species are at local extinctions. Exclusion, the equilibria where one species is at a positive equilibrium and the other is at a local extinction, models the system before an invasion. Coexistence represents a successful invasion in which the introduced species has established itself and both species reach a new equilibrium. The paper then moves to the single species non-linear system, analyzing equilibria using computational homology before computing a basin of attraction for small neighborhoods around each attracting equilibrium. This approach to studying the non-linear model provides more a global description of dynamics. The basins of attraction discussed more fully in the paper give us an approximation of which initial populations will move toward the equilibria of choice.

In the interest of maintaining a mathematical focus, no specific species are used in this paper. However, we see from the scientific literature that the Lefkovitch

matrix model used in this paper and related models such as the Leslie and Lewis models are widely used in population modeling. For example, Leslie matrices have been used to model the effects of elevation on mosquito populations and the effects of turtle excluder devices on loggerhead sea turtles [2, 6].

This paper is motivated by the competition (Lefkovitch) model between two species. However, the two species model is in four dimensions and is therefore hard to construct and visualize with no background. Thus, the paper focuses on the two-dimensional single species model to refine and illustrate the techniques used for analysis and building the basins of attraction. We expect the methods described here to be immediately applicable to the higher dimension Lefkovitch model and other population models found in the literature.

Chapter 2

Stage Structured Populations

2.1 Life Cycle

Each population in our model is divided by developmental stage. Although the Lefkovitch model we use in Chapter 3 allows any number of stages, we chose to divide the species into two stages, juveniles (sexually immature individuals) and adults (sexually mature individuals). We let n_1 be the number of juveniles and n_2 be the number of adults. Each stage has a rate of survival, s and p respectively, between 0 and 1. Of the juvenile survivors, some proportion m mature to adulthood, while $(1 - m)$ remain in the juvenile stage in a single time step. Let F represent the fertility rate [15]. The life cycle is illustrated in Figure 2.1.

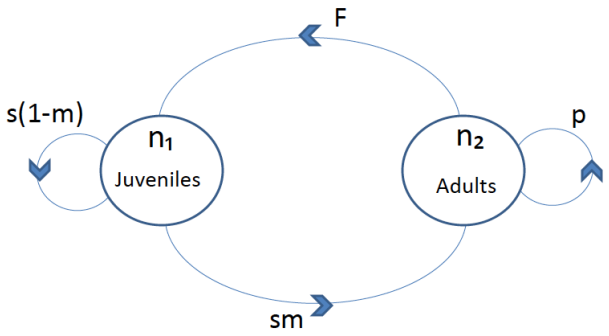

Figure 2.1: Staged population life cycle

Division by developmental stage allows individuals to stay in the same stage for multiple time steps. Thus, parameter values like survivorship are based on characteristics like size, which is often more realistic than an age-structured model. Both the age- and stage-structured models have difficulties when applied to species with continuous reproduction. This model inherently includes pulse reproduction;

reproduction takes place at the beginning of each time step. Thus, a time step should be chosen such that the population will reproduce once in each interval. Pulse reproduction makes this model a good fit for species like fish with a short spawning season but not for species with a year-round reproductive season [16]. It is common to restrict the population size to the number of females. Limiting the counted population to females allows individuals to mate outside of their stage without complicating the fertility rate [13].

Throughout nature, species have developed different strategies for survival and reproduction known as *life history strategies*. For this model, we focus on varying maturation rates, m, and adult survival, p, to divide populations into differing life history strategies. We differentiate between large and small values for m and p creating species with the following descriptions:

(i) Precocious (m large): individuals mature quickly;

(ii) Delayed (m small): long juvenile period, individuals reproduce late in life;

(iii) Iteroparous (p large): adults live for many generations, reproducing multiple times; and

(iv) Semelparous (p small): adults live for a short time and reproduce only once [15].

By pairing the different magnitudes of maturation and survival rates we produce four classifications of species. Since we do not use any specific species in the study, we assigned parameter values that would clearly differentiate between the categories. Changing these values to reflect actual populations does not change the implementation of the model. The parameters that we chose are listed in Table 2.1.

Table 2.1: Life History Strategies

Case	s	p	m	classification
1	0.9	0.1	0.1	delayed semelparous
2	0.9	0.1	0.9	precocious semelparous
3	0.9	0.9	0.1	delayed iteroparous
4	0.9	0.9	0.9	precocious iteroparous

Delayed semelparous species include periodical cicadas and some species of periodically-flowering bamboo. These species take many years to reach maturity, and then only reproduce once. Precocious semelparous species are more common and include many insects and spiders as well as annual plants. Many large mammals like humans and whales as well as some birds such as albatrosses are delayed

iteroparous and are characterized by slow maturation and long reproductive periods. Small mammals and birds are usually percocious iteroparous; they start reproducing early, around a year or less of age, but reproduce multiple times over several years [15].

2.2 Density Dependence

Density dependence in system parameters may limit population size as a population grows. This kind of mechanism is found throughout nature as a carrying capacity on species. Usually, density dependence is only noticeable with respect to some limiting factor like food or habitat. Different limiting factors affect life history parameters in different ways. With very distinct juvenile and adult stages, like in toads, where the individuals of each stage live in separated habitats, isolated habitat degradation can impact the survival of one stage much more than the other. In this model, the distinction between juveniles (n_1) and adults (n_2) allows us to model competition between the adults of one species and juveniles of another species or between the adults of both populations or any other combination of stages. Division into stages also allows models to express intraspecific competition between different stages of the same species [9]. Species with complex life cycles that undergo a metamorphosis often do not demonstrate any competition between juveniles and adults whereas species not undergoing metamorphosis more often compete across the stage division [9].

Each life history parameter in the model can be made density dependent, meaning it is a function of population size n_1 and/or n_2. For this study, we made fertility dependent on the density of the adult population.

In the single species model density dependent fertility is incorporated into the model to limit the population size. We use the Beverton-Holt density dependence function[5, equation 16.12]. The fertility rate is:

$$F(n_2(t)) = \frac{\alpha}{1 + \beta n_2(t)}, \tag{2.1}$$

where α is the maximum fertility rate of the population. The fertility rate will approach α when $n_2(t)$ is very small. As $n_2(t)$ grows, the fertility rate declines to avoid overpopulation and reflect crowding effects. Scaling n_2, β determines the strength of density dependence. The Beverton-Holt and Ricker functions are used most often to model density dependence.

In the two species model, density dependent fertility not only limits the size of the population, but also expresses competition for resources between the native and invading populations. The fertility rate will fall as either population grows.

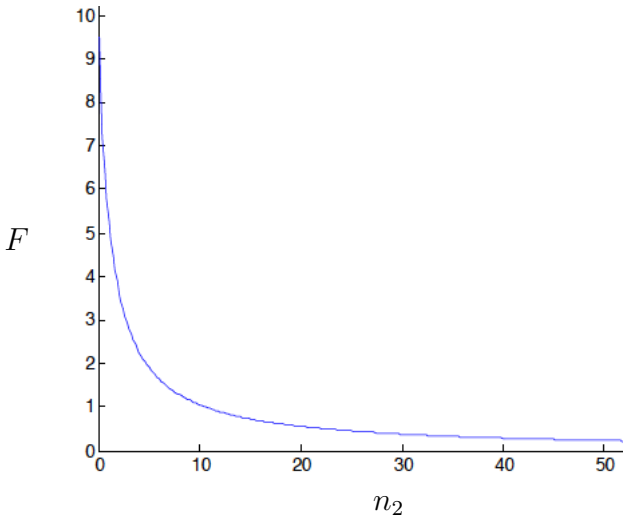

Figure 2.2: Fertility rate given $\alpha = 9.5$ and $\beta = 0.8$

Density dependence on two species is expressed through a similarly structured fertility function with dependence on both adult populations:

$$F_1(n(t)) = \frac{\alpha_1}{1 + \beta_{11} n_2(t) + \beta_{21} n_4(t)}. \tag{2.2}$$

Chapter 3

Competition Model

3.1 Lefkovitch Matrix

Since their development in the 1940s, matrix-based models of population dynamics have become a common tool for modeling populations with an age or stage delineated structure [4]. Lewis and Leslie pioneered the field using age structured models. In these models, once a time step is chosen (i.e., a year, a month, or a week), each individual changes age groups for each iteration of the time step [13, 12]. In the mid-1960s, the Lefkovitch matrix model improved on existing population modeling techniques by allowing populations to exhibit staged life cycles where individuals are promoted from one stage to the next based on developmental characteristics instead of time steps. The Lefkovitch model is often used as an alternative to the Leslie matrix model.

The population is written as a vector that reflects the proportional division of the population stages:

$$\mathbf{n}(t) = \begin{bmatrix} n_1(t) \\ n_2(t) \end{bmatrix}. \tag{3.1}$$

The Lefkovitch model organizes the parameters from the life cycle graph from Figure 2.1 into a matrix, $\mathcal{A}(\mathbf{n})$. In the literature, it is common to call $\mathcal{A}(\mathbf{n})$ simply $\mathcal{A}$ or some other letter. We avoid this notation because it suppresses the mathematical dependence of the fertility term on the adult population size. Since fertility is a parameter value, it is easy to forget that it is a function instead of a constant. We find the reminder that the Lefkovitch matrix depends on the population size to be helpful.

Lefkovitch matrices can easily be expanded to represent species with many stages. The main diagonal of $\mathcal{A}(\mathbf{n})$ contains the rates at which each stage persists

into the next generation. The subdiagonal is the maturation rate to the next stage and the top row is the fertility rate at each stage [18]. More generally, the matrix entry a_{ij} is the rate at which individuals move from stage j to stage i. The matrix format makes it easy to represent individuals skipping stages and reproducing from any stage. This flexibility makes it widely applicable to species with diverse life histories. For the two stage model described above, the Lefkovitch matrix is

$$\mathcal{A}(\mathbf{n}) = \begin{bmatrix} s_1(1-m_1) & F_1(n) \\ s_1 m_1 & p_1 \end{bmatrix}. \tag{3.2}$$

Multiplication of the Lefkovitch matrix by a population vector yields the population vector of the next generation:

$$\mathbf{n}(t+1) = \mathcal{A}(\mathbf{n}(t))\mathbf{n}(t). \tag{3.3}$$

At equilibrium, $\mathbf{n}^* = \mathcal{A}(\mathbf{n}^*)\mathbf{n}^*$.

Now consider the mapping from one time step to the next, $f : \mathbb{R}^k \to \mathbb{R}^k$, given by $f(\mathbf{x}) = \mathcal{A}(\mathbf{x})\mathbf{x}$. This mapping will take the population vector $\mathbf{n}$ and, using the Lefkovitch matrix dependent on that vector, find the population at the next time step.

Definition 3.1.1 (Trajectory)**.** *[7] Given $f : \mathbb{R}^k \to \mathbb{R}^k$. A trajectory through $x \in \mathbb{R}^k$ is a sequence $\gamma_{x_0} := (\ldots, x_{-1}, x_0, x_1, \ldots)$ such that $x_0 = x$ and $x_{b+1} = f(x_b)$ for all $n \in \mathbb{Z}$.*

The definition above is for a full trajectory. A forward trajectory would only consist of $\gamma_{x_0} := (x_0, x_1, ...)$ and a backward trajectory would, predictably, be $\gamma_{x_0} := (..., x_{-1}, x_0)$. Given that the model is non-invertible, there can be infinitely many backwards trajectories in some cases, but the forwards trajectory is uniquely determined by the Lefkovitch matrix.

3.2 Two Species Model

We can expand this model to show competition between two species. Both species in this model have two life cycle stages and density dependent fertility. Table 3.1 shows the notation to differentiate between the two species.

The population vector now includes the values for each stage of both species,

$$\mathbf{n}(t) = \begin{bmatrix} n_1(t) \\ n_2(t) \\ n_3(t) \\ n_4(t) \end{bmatrix}. \tag{3.4}$$

Table 3.1: Two Species Model

	Species 1	Species 2
juvenile population	n_1	n_3
adult population	n_2	n_4
juvenile survival	s_1	s_2
adult survival	p_1	p_2
maturity rate	m_1	m_2
fertility	F_1	F_2

The Lefkovitch matrix for two species is built using the individual species' matrices to make a block diagonal matrix that we will continue to call $\mathcal{A}(\mathbf{n})$.

$$\mathcal{A}(\mathbf{n}) = \begin{bmatrix} s_1(1-m_1) & F_1(\mathbf{n}) & 0 & 0 \\ s_1 m_1 & p_1 & 0 & 0 \\ 0 & 0 & s_2(1-m_2) & F_2(\mathbf{n}) \\ 0 & 0 & s_2 m_2 & p_2 \end{bmatrix},$$

where the fecundity rates F_1 and F_2 are

$$F_1(\mathbf{n}) = \frac{\alpha_1}{1+\beta_{11}n_2+\beta_{21}n_4}$$

and

$$F_2(\mathbf{n}) = \frac{\alpha_2}{1+\beta_{12}n_2+\beta_{22}n_4}.$$

Just as before, multiplication of the Lefkovitch matrix by the population vector will result in the population of the next time step:

$$\mathcal{A}\mathbf{n}(t) = \mathbf{n}(t+1).$$

The Lefkovitch matrix and population vector can be written as a set of difference equations. The two species model is a four-dimensional discrete dynamical system:

$$n_1' = f_1(\mathbf{n}) = s_1(1-m_1)n_1 + \frac{\alpha_1}{1+\beta_{11}n_2+\beta_{21}n_4}n_2, \tag{3.5}$$

$$n_2' = f_2(\mathbf{n}) = s_1 m_1 n_1 + p_1 n_2, \tag{3.6}$$

$$n_3' = f_3(\mathbf{n}) = s_2(1-m_2)n_3 + \frac{\alpha_2}{1+\beta_{12}n_2+\beta_{22}n_4}n_4, \tag{3.7}$$

$$n_4' = f_4(\mathbf{n}) = s_2 m_2 n_3 + s_2 n_4. \tag{3.8}$$

These equations will be used later to find the population size at equilibrium.

3.3 Choosing α and β Parameter Values

We next choose parameter values for α and β. The maximum fertility rate α and the strength of density dependence β are determined by the species in question. Since this study does not name specific species, we decided on reasonable values for α and β that can be adjusted when the model is applied.

Before choosing a value for α, we must first clarify the constraints on α. Clearly, α must be greater than or equal to any other fertility rate achieved by the population. The single species model can be expressed through two difference equations calculating the population in the next time step:

$$n_1' = f_1(\mathbf{n}) = s_1(1-m_1)n_1 + \frac{\alpha_1}{1+\beta_{11}n_2}n_2 \tag{3.9}$$

$$n_2' = f_2(\mathbf{n}) = s_1 m_1 n_1 + p_1 n_2. \tag{3.10}$$

Analytically solving these equations to find equilibria, we find the trivial equilibrium and the nontrivial equilibrium where

$$n_1^* = \frac{1-p_1}{s_1 m_1} n_2^* \tag{3.11}$$

$$n_2^* = \left(\frac{s_1 m_1 \alpha_1}{(1-p_1)(1-s_1(1-m_1))} - 1\right)\frac{1}{\beta_{11}}. \tag{3.12}$$

From the original Beverton-Holt equation, Equation 2.1, we see that the maximum fertility rate occurs when the population is very small. This is shown graphically in Figure 2.2. Solving the second equation for $n_2 = 0$ we can find a lower limit on α which we call α_L. When $\alpha = \alpha_L$ there is only one equilibrium point, the trivial solution. When α drops below a α_L, the equilibrium values of n_2 and therefore n_1 will be negative and biologically irrelevant for our model. Each of the four cases in Table 2.1 has a different α_L that depends on the life history parameter values. Table 3.2 shows α_L for each of the four cases.

Table 3.2: Lower limit of α for positive nontrivial solution

Case	classification	s	p	m	α_L
1	delayed semelparous	0.9	0.1	0.1	1.9
2	precocious semelparous	0.9	0.1	0.9	1.0111
3	delayed iteroparous	0.9	0.9	0.1	0.2111
4	precocious iteroparous	0.9	0.9	0.9	0.1123

When $\alpha = \alpha_L$, the only equilibrium is the extinction equilibrium. Raising α slightly above that level will result in a small nontrivial equilibrium population. We can raise α quite a bit higher and raise the nontrivial equilibrium. The question that remains is: how large should α be? The good news about this question is that, in this model, it does not matter. The population vector found in the Lefkovitch model will return the ratio of juveniles to adults. Even if the numbers in the vector are not the actual population numbers, they will still exhibit the same proportional relation. The exact number returned depends on the values of α and β, but when α and β change, the ratio will the remain the same. From Equation 3.12, we see that n_2 is dependent on α and β, but n_1, Equation 3.11, will have the same relationship to n_2 no matter what α and β are since $\frac{n_1^*}{n_2^*} = \frac{1-p_1}{s_1 m_1}$. Since the value of α does not influence the behavior of the model as long as $\alpha > \alpha_L$, we set $\alpha = 5\alpha_L$.

The β parameter determines the extent of density dependence. Given our selection of α and the information found in [11], it follows that in order to have a stable coexistence, $\beta_{12} < \beta_{11}$ and $\beta_{21} < \beta_{22}$. These inequalities are derived from more general inequalities. The specific inequalities in this paper are conditions for stability given our method of choosing α. They make sense intuitively because individuals from the same population are likely to occupy the same niche and experience heavy intra-specific competition while individuals from different populations may inhabit overlapping, but not identical niches and not compete as closely. For the development of this model, we chose $\beta_{ii} = .8$, and $\beta_{ij} = .6$.

Chapter 4

Fixed Points

4.1 Linearization

For the first analysis of the dynamics of the model, we linearized around the equilibria and determined stability. In order to linearize the system, we calculated the Jacobian, J, which is the matrix of partial derivatives

$$J = \left[\begin{array}{c} \frac{\partial f_i(\mathbf{n})}{\partial n_j} \end{array} \right]_{ij}.$$

Where $f_i(\mathbf{n})$ is an equation from the four dimensional system found in Equations 3.5 through 3.8.

Computing J for the two species model, we find

$$J = \left[\begin{array}{cccc} s_1(1-m_1) & \frac{(1+\beta_{11}n_2+\beta_{21}n_4)\alpha_1-\alpha_1\beta_{11}n_2}{(1+\beta_{11}n_2+\beta_{21}n_4)^2} & 0 & \frac{-\alpha_1\beta_{21}n_2}{(1+\beta_{11}n_2+\beta_{21}n_4)^2} \\ s_1m_1 & p_1 & 0 & 0 \\ 0 & \frac{-\alpha_2\beta_{12}n_4}{(1+\beta_{12}n_2+\beta_{22}n_4)^2} & s_2(1-m_2) & \frac{(1+\beta_{12}n_2+\beta_{22}n_4)\alpha_2-\alpha_2\beta_{22}n_4}{(1+\beta_{12}n_2+\beta_{22}n_4)^2} \\ 0 & 0 & s_2m_2 & p_2 \end{array} \right]$$

To continue the analysis, we evaluated J at each equilibrium. In order to find the stability of the fixed point, we need only look at the eigenvalues of J. Using the following theorem, we can determine the stability of the equilibrium points.

Theorem 4.1.1. *[3] Let* $= (\mathbf{f_1}, \mathbf{f_2}, ..., \mathbf{f_k})$ *be a map on* $\mathbb{R}^k$*, and let* $\boldsymbol{x} \in \mathbb{R}^k$*. Let* $\boldsymbol{Df}(\boldsymbol{x})$ *denote the Jacobian of* $\boldsymbol{f}$ *at* $\boldsymbol{x}$*. Assume* $\boldsymbol{f}(\boldsymbol{x}) = \boldsymbol{x}$*.*

1. *If the magnitude of each eigenvalue of* $\boldsymbol{Df}(\boldsymbol{x})$ *is less than* 1*, then* $\boldsymbol{x}$ *is a sink.*
2. *If the magnitude of each eigenvalue of* $\boldsymbol{Df}(\boldsymbol{x})$ *is greater than* 1*, then* $\boldsymbol{x}$ *is a source.*

When the leading eigenvalue is less than 1, we see that the fixed point is *asymptotically stable*.

Definition 4.1.2 (asymptotically stable)**.** *A fixed point, x, is* asymptotically stable *if it belongs to the interior of its stable set, i.e., if there is $\delta > 0$ such that $lim_{n\to\infty} d(f^n(x), f^n(y)) = 0$ whenever $d(x, y) < \delta$.*

When the leading eigenvalue is greater than 1, the fixed point may be a source, if all of the eigenvalues are greater than one, or a saddle, if the other eigenvalue(s) are less than one. What is important for this model is that if the leading eigenvalue is greater than 1, the fixed point will be unstable.

First, we consider the two-dimensional model. With the chosen parameters, we can find the non-trivial equilibrium where both the juvenile and adult populations are positive. The nontrivial equilibria for each case of the two dimensional system are in Table 4.1.

Table 4.1: Fixed points for all cases

Case	trivial	non-trivial
1	$(0, 0)$	$(50, 5)$
2	$(0, 0)$	$(5.5556, 5)$
3	$(0, 0)$	$(5.5556, 5)$
4	$(0, 0)$	$(0.6173, 5)$

Linearizing around these equilibria and checking the leading eigenvalue of the Jacobian may yield the stability type. For the two-dimensional model of Case 1 we have eigenvalues of 1.4455 and -0.5355 for the trivial equilibrium and eigenvalues of 0.8553 and 0.0547 for the non-trivial equilibrium. From this we see that the trivial equilibrium will be unstable and the non-trivial equilibrium will be stable. This trend persists in the other species when modeled alone. Table 4.2 lists the dominant eigenvalue, λ_{max}, for each equilibrium.

Table 4.2: Dominant eigenvalues: two-dimensional

Case	trivial	non-trivial
1	1.4455	0.8553
2	2.1186	0.4998
3	1.1665	0.9313
4	1.2818	0.9219

The same analysis can be undertaken for the four-dimensional model. With four cases, we can have ten competition instances. Each instance will have four

equilibrium: 1) extinction, where both populations are extinct, 2) exclusion 1, where population 1 is at a nontrivial equilibrium and population 2 is extinct, 3) exclusion 2, where population 2 is at a nontrivial equilibrium and population 1 is extinct, and 4) coexistence, where both populations are nontrivial. Table 4.3 shows λ_{max} for each equilibrium.

Table 4.3: Dominant Eigenvalues: four-dimensional model

Cases	extinction	exclusion 1	exclusion 2	coexistence
1 vs 1	1.4455	1.0379	1.0379	0.9818
1 vs 2	2.1186	1.1068	1.0379	0.9738
1 vs 3	1.4455	1.0155	1.0379	0.9894
1 vs 4	1.4455	1.0220	1.0379	0.9869
2 vs 2	2.1186	1.1068	1.1068	0.9467
2 vs 3	2.1186	1.0155	1.1068	0.9874
2 vs 4	2.1186	1.0220	1.1068	0.9837
3 vs 3	1.1665	1.0155	1.0155	0.9923
3 vs 4	1.2818	1.0220	1.0155	0.9912
4 vs 4	1.2818	1.0220	1.0220	0.9896

In the four-dimensional model, the trivial and exclusion equilibria will be unstable and the coexistence equilibrium will be stable.

4.2 Outer Enclosures and Topological Methods

The linearization techniques used in Chapter 4.1 give us useful information about the stability of the equilibrium points. However, this information is limited in scope to a sufficiently small neighborhood around each point. Computational topology offers another way for us to verify the existence and analyze the stability of the equilibrium points in the non-linear system. Motivated by this computational approach, we will extend our techniques in order to gain a more global picture of the dynamics. Towards this goal, we develop computational algorithms to compute basins of attraction for neighborhoods of stable equilibria.

The overarching goal of this paper is to compute basins of attraction for (isolating) neighborhoods of attracting equilibrium points. We begin by defining *isolating neighborhood* and discuss how they are used in detecting equilibria and their stability. We then explain the algorithm for computing basins for attraction for attracting isolating neighborhoods.

To begin studying the system, we first compute an *outer enclosure* for the map $f : \mathbb{R}^k \to \mathbb{R}^k$ on a compact region of $\mathbb{R}^k$. This outer enclosure will be a

representation of the system that we can store and manipulate in the computer. The compact region will be a closed and bounded subset of $\mathbb{R}^k$ in which we study the dynamics. The choice of phase space where we will build an outer enclosure is called a *root box* and for our purposes is given as an explicit box (product of closed intervals) in the phase space.

Since we already know the numerical values of the equilibria, listed in Table 4.1, we create root boxes for each case containing these equilibria and the portion of the biologically relevant area around them that we would like to study. In particular, we will not include negative populations. The root box will be subdivided into a grid, $\mathcal{G}$. Let the rectangular set $W = \prod_{k=1}^{n}[x_k^-, x_k^+] \subset \mathbb{R}^n$ be the root box that we will partition into a *cubical grid*

$$\mathcal{G}^{(d)} := \left\{ \prod_{k=1}^{n} \left[x_k^- + \frac{i_k r_k}{2^d}, x_k^- + \frac{(i_k+1)r_k}{2^d} \right] \Big| i_k \in 0, \ldots, 2^d - 1 \right\}$$

where $r_k = x_k^+ - x_k^-$ is the radius of W in the kth coordinate and the depth d is a nonnegative integer. We call an element of the grid, $B = \prod_{k=1}^{n} \left[x_k^- + \frac{i_k r_k}{2^d}, x_k^- + \frac{(i_k+1)r_k}{2^d} \right]$, a *box* [7]. We let $|B|$ represent a grid element as a subset of phase space. We use the software package GAIO (which stands for Global Analysis of Invariant Objects) to create the grid at depth d [8]. GAIO uses a MATLAB interface and the remaining computations will be carried out in MATLAB.

The grid, $\mathcal{G}$, specifies a computational resolution at which to view the map $\mathcal{F}$. Instead of mapping an initial condition forward in time from point to point, we can consider one box of the grid, B_0, and find which boxes it maps into. All boxes that may contain any part of the image of B_0 under the mapping f will be contained in the constructed image $\mathcal{F}(B_0)$ on the grid.

More specifically, we will construct a *multivalued map* $\mathcal{F} : \mathcal{G} \rightrightarrows \mathcal{G}$, where $\mathcal{F}(B) \subseteq \mathcal{G}$ for $B \in \mathcal{G}$. We refer to $\mathcal{F}$ as *multivalued* because the image under $\mathcal{F}$ of a single input $B \in \mathcal{G}$ is a subset of $\mathcal{G}$ rather than a single object in $\mathcal{G}$. This representation of the map on the grid creates an *outer enclosure* of the true image. This representation should incorporate all (bounded) errors so we also think of it as outer bounds on the images of the map. The requirement that $\mathcal{F}$ be an outer enclosure may then be given as follows for $B, G \in \mathcal{G}$. We see that $G \in \mathcal{F}(|B|)$ whenever $f(|B|)$ intersects $|G|$ and $|\mathcal{F}(B)|$ is *acyclic*, meaning it has the topology of a point.

For our study, we construct $\mathcal{F}$ by using *Lipschitz bounds* on images of f.

Definition 4.2.1 (Lipschitz)**.** *For $N \subseteq \mathbb{R}^k$, $f : N \to \mathbb{R}$ is said to be* Lipschitz *on*

N if there exists L such that

$$||f(\boldsymbol{v}) - f(\boldsymbol{w})|| \leq L||\boldsymbol{v} - \boldsymbol{w}||$$

for all $\boldsymbol{v}, \boldsymbol{w} \in N$. If it exists, the constant L is called a Lipschitz constant *for f on N.*

To compute the image of B, we can think of the grid element B as a box with a center $\mathbf{c} \in \mathbb{R}^k$ and radius $\mathbf{r} \in \mathbb{R}^k$ that can be expressed as

$$B = \mathbf{c} + \begin{bmatrix} r_1[-1,1] \\ r_2[-1,1] \\ \vdots \\ r_k[-1,1] \end{bmatrix}.$$

This leads to

$$f(|B|) \subseteq f(\mathbf{c}) + L \begin{bmatrix} r_1[-1,1] \\ r_2[-1,1] \\ \vdots \\ r_k[-1,1] \end{bmatrix} = \tilde{f}(|B|)$$

where L is a Lipschitz constant for f on $|B|$. This produces a bounding box, $\tilde{f}(|B|)$, for the image $f(|B|)$, which is then intersected with the grid $\mathcal{G}$ to produce the outer enclosure image. The map $\mathcal{F}$ is defined as

$$\mathcal{F}(|B|) := \left\{ G \in \mathcal{G} : |G| \cap \left(f(\mathbf{c}) + L \begin{bmatrix} r_1[-1,1] \\ r_2[-1,1] \\ \vdots \\ r_k[-1,1] \end{bmatrix} \right) \neq \emptyset \right\}.$$

Following this approach $\mathcal{F}$ is an outer enclosure up to possible machine error in computations. We expect that machine error will be very small and not impact the results in any significant way. In the next implementation phase, we plan to incorporate machine round off to verify this. This representation, $\mathcal{F}$ can be stored in a sparse matrix $P = [p_{ij}]_{ij}$, where $p_{ij} = 1$ when $B_i \in \mathcal{F}(B_j)$ and $p_{ij} = 0$ otherwise.

Now that we have built a representation we give the definitions necessary to define Conley Index theory which we will use to analyze the dynamics encoded by the outer enclosure.

Definition 4.2.2 (Maximal Invariant Set)**.** *[8] The maximal invariant set con-*

tained in a set $Q \subseteq M$ is defined as

$$\mathrm{Inv}(Q) = \{x \in Q : \text{ there exists } \gamma_x \subset Q\}$$

where γ_x is a full trajectory through x as defined in Definition 3.1.1.

Figure 4.1 shows a covering of the maximal invariant set in the root box of the two-dimensional model of a population of Case 1.

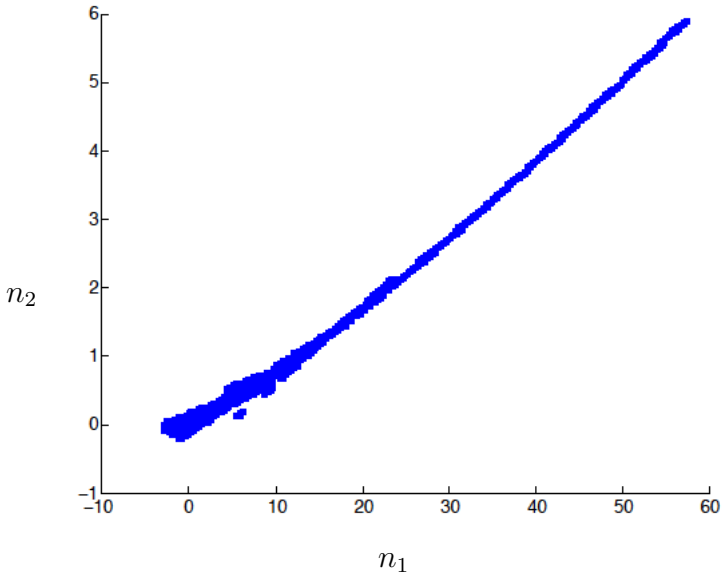

Figure 4.1: Maximal invariant set of Case 1 at depth 16

Definition 4.2.3 (Isolating Neighborhood)**.** *[7] A compact set $N \subset \mathbb{R}^n$ is an* isolating neighborhood *if*

$$\mathrm{Inv}(N, f) \subset N^\circ \tag{4.1}$$

where N° denotes the interior of N. S is an isolated invariant set *if $S = \mathrm{Inv}(N, f)$ for some isolating neighborhood N.*

Figure 4.2 depicts an example of an isolating neighborhood. Isolating neighborhoods are computable given an appropriate outer enclosure, but we will not delve into the algorithm here. For details on that algorithm see [8]. Isolating neighborhoods are the building blocks of *Conley Index theory*. We use the next two definitions for background building up to the definition of the Conley Index.

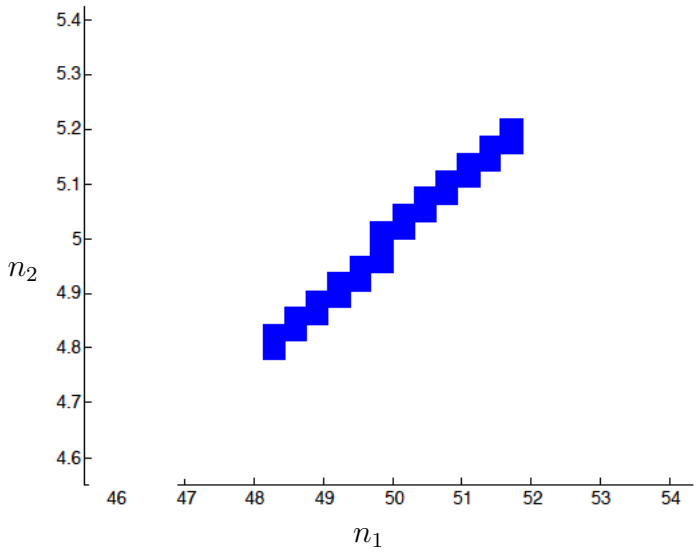

Figure 4.2: An isolating neighborhood containing the non-trivial equilibrium in Case 1 at depth 16.

Definition 4.2.4. *Let $P = (P_1, P_0)$ be a pair of compact sets with $P_0 \subset P_1 \subset X$. The map induced on the pointed quotient space $(P_1/P_0, [P_0])$ is*

$$f_P(x) := \begin{cases} f(x) & \text{if } x, f(x) \in P_1 \setminus P_0 \\ [P_0] & \text{otherwise.} \end{cases} \tag{4.2}$$

Definition 4.2.5. *([7]) The pair of compact sets $P = (P_1, P_0)$ with $P_0 \subset P_1 \subset X$ is an* index pair *for f provided that*

1. *the induced map, f_P, is continuous,*
2. *$\overline{P_1 \setminus P_0}$, the closure of $P_1 \setminus P_0$, is an isolating neighborhood.*

In this case, we say that P is an index pair for the isolated invariant set $S = \mathrm{Inv}(\overline{P_1 \setminus P_0}, f)$.

On an isolating neighborhood, I, building an index pair involves computing P_0 since P_1 will be constructed as the union of I and P_0. In this study, P_0 is also known as the *exit set* for I. The exit set records the portion of the boundary of I corresponding to the directions in which a trajectory may leave the isolating neighborhood. If the exit set is empty, then once a trajectory enters the isolating neighborhood, it does not leave.

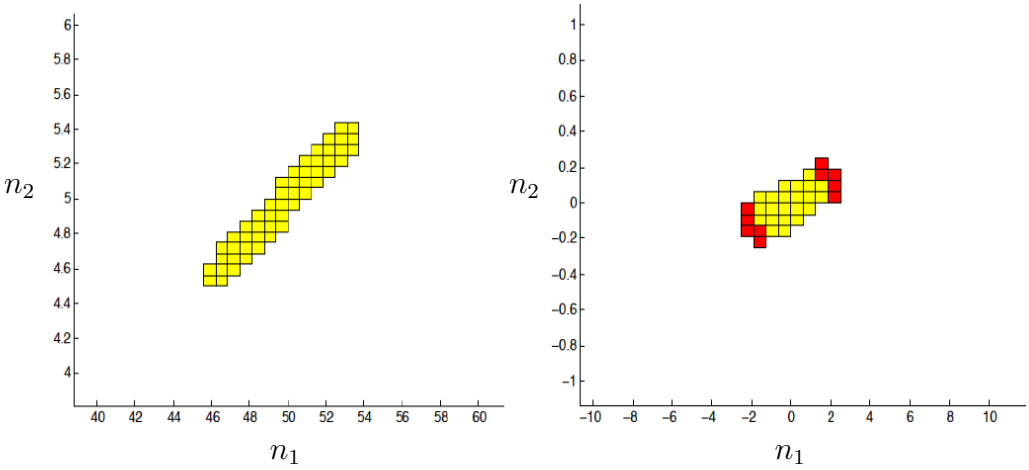

Figure 4.3: Index pairs for Case 1 at depth 14 around non-trivial and trivial equilibria respectively. The yellow (lighter) regions are isolating neighborhoods and the red (darker) region is the exit set for the second index pair. The exit set for the first index pair is empty.

The following technical definition is required for the formal definition of the Conley index.

Definition 4.2.6. *Two group homomorphisms, $\phi : G \to G$ and $\psi : G' \to G'$ on abelian groups G and G' are* shift equivalent *if there exist group homomorphisms $r : G \to G'$ and $s : G' \to G$ and a constant $m \in \mathbb{N}$ (referred to as the 'lag') such that*

$$r \circ \phi = \psi \circ r, \quad s \circ \psi = \phi \circ s, \quad r \circ s = \psi^m, \quad \text{and} \quad s \circ r = \phi^m.$$

The shift equivalence class of ϕ, *denoted $[\phi]_s$, is the set of all homomorphisms ψ such that ψ is shift equivalent to ϕ.*

Definition 4.2.7. *Let $P = (P_1, P_0)$ be an index pair for the isolated invariant set $S = \mathrm{Inv}(\overline{P_1 \setminus P_0}, f)$ and let $f_{P*} : H_*(P_1, P_0) \to H_*(P_1, P_0)$ be the map induced on the relative homology groups $H_*(P_1, P_0)$ from the map f_P. The* Conley index of S *is the shift equivalence class of f_{P*}*

$$\mathrm{Con}(S, f) := [f_{P*}]_s. \tag{4.3}$$

The Conley Index is an algebraic topological index for isolated invariant sets. We have an unfair advantage because we have already analytically solved the equations for the equilibria. Without knowing the equilibria, the Conley Index may be able to detect fixed points contained in isolated invariant sets. Indeed,

this is the case for all of the equilibria we have considered in all cases. The most important property of the Conley Index for our purposes is that it's computable from the outer enclosure [7]. For our work, we use previously developed MATLAB algorithms for computing index pairs ([7]) and a computational homology package called CHomP to compute the index [1].

For our studies, a representation of the shift equivalence class for the Conley Index is a finite number of nonzero matrices, each of which represents a group homomorphism on a level of homology.

Definition 4.2.8. *Let S be an isolated invariant set. The* Lefschetz number of S *is defined as*

$$L(S, f) := \sum_k (-1)^k (f_{Pk}), \tag{4.4}$$

where $P = (P_1, P_0)$ is an index pair for S and f_{P_k} is the map induced by f_P on the kth level of homology.

The Lefschetz number is essential to the following theorem and its corollary.

Theorem 4.2.9. *Let S be an isolated invariant set. If*

$$L(S, f) \neq 0, \tag{4.5}$$

then S contains a fixed point.

Using this theorem, we can verify the existence of equilibria in isolating neighborhoods with nonzero Lefchetz numbers. Note that this does not require first analytically solving for the equilibria.

For the first index pair depicted in Figure 4.3 in which the empty set is empty, the relative homology will record the topology of a disc (the isolating neighborhood) and a disconnected point (the null set representing the exit set). In this case, the relative homology groups and induced maps on homology are

$$H_0(P_1, P_0) = \mathbb{Z}, f_{P0} = \begin{bmatrix} 1 \end{bmatrix},$$

$$\text{and } H_k(P_1, P_0) = 0, f_{Pk} = 0, \text{ when } k \neq 0$$

where $f_{Pk} : H_k(P_1, P_0) \to H_k(P_1, P_0)$.

For the index pair for the isolating neighborhood of the trivial equilibrium depicted in Figure 4.3, the relative homology of the index pair and maps on homology are

$$H_1(P_1, P_0) = \mathbb{Z}, f_{P1} = [1]$$

$$H_k(P_1, P_0) = 0, f_{Pk} = 0, \text{ where } k \neq 1.$$

This homology information was computed using the software CHomP [1]. When we use this analysis at higher dimensions we rely more on the interpretation of the index since pictures are less helpful.

Chapter 5

Basins of Attraction

Linearizing the system to analyze the equilibrium points gives us limited information about the system's dynamics. While the analysis close the equilibrium can tell us the local stability and limiting behavior, it does not give us the global information to predict asymptotic behavior for a large class of initial conditions. Furthermore, global information adds to biological relevance of the model. The model itself may break down close to the equilibria because populations are measured in discrete increments while the linearization is only applicable very close to the equilibrium. Therefore, to gain a understanding of the global dynamics of the system, we use the non-linear model to compute basins of attraction.

The goal of this analysis is that knowledge of the basins of attraction will allow biologists to utilize the methods presented to follow cost effective conservation techniques. If a population can be managed until it is in the basin of attraction, the dynamics of the system should naturally move it to the non-trivial equilibrium. On the other hand, if conservationists want to drive out a species, it will have to be controlled at least to the point where it exits the basin of attraction, if not all the way to extinction.

Now that we have examined the eigenvalues of the linearized system and the Conley Index of the non-linear system we move on to computing the basins of attraction around the attracting nontrivial equilibrium. For this research, we used GAIO, introduced in the last chapter, to implement the algorithms presented here. Starting with the two-dimensional (one population, two stage) model, we first analytically find the fixed points which are given in Table 4.1.

Following the process in Chapter 4.2, we construct a root box, used to initialize a tree in GAIO, that includes all of the fixed points. This time, we do not find the maximal invariant set. The maximal invariant set was helpful before to limit the area in consideration and thereby make calculations more efficient, but now we want to find the area of the root box that moves towards the isolating

neighborhood, so the entire box must be subdivided and considered.

It should be noted that basins of attraction can only be computed around attracting isolating neighborhood. An attracting isolating neighborhood is one in which the exit set is empty. The isolating neighborhoods around unstable equilibria will have exits sets through which a trajectory can leave even if it has entered the neighborhood.

We use the following algorithm to compute the basins.

Compute Basin of Attraction

```
INPUT:  grid 𝒢, combinatorial enclosure ℱ on 𝒢, attracting
        isolating neighborhood ℐ
OUTPUT: a basin of attraction ℬ for the isolated
        neighborhood ℐ

ℬ = compute_basin(𝒢, ℱ, ℐ)
    Set ℬ := ℐ;
    Set flag to stop
    Find ℱ^{-1}(ℬ) = 𝒞, where ℱ^{-1}(ℬ) = {c : ℱ(c) ∈ ℬ}
    Let 𝒞 = 𝒞 \ ℬ
    For each c ∈ 𝒞, if ℱ(c) ⊆ ℬ then ℬ = ℬ ∪ {c}
    If elements were added to ℬ, change flag to continue
    If flag is set to continue, repeat the algorithm starting
        with set flag to stop
```

At each depth, the computed basin is a lower bound or inner approximation of the true basin. We note that refining the resolution of the grid leads to a larger computed basin. There is a trade-off between computation expense and basin error. This means that the basin generated by this algorithm is dependent on the depth of subdivision of the root box. The next two images illustrate this phenomenon.

Figure 5.1 A shows the basin of attraction for the nontrivial equilibrium of Case 1. After 10 subdivisions it covers 95.31% of the root box. Dividing to a depth of 14, Figure 5.1 B, the isolating neighborhood around the non-trivial equilibrium shrinks, but the basin of attraction grows to cover 99.94% of the root box. In the figure, the dark section in the middle of the image is the isolating neighborhood around the nontrivial equilibrium, the light section is the basin of attraction, and the dark boxes in the corner next to the origin are the portion of the root box not contained in the basin. If we divide still further, the boundary of the basin will continue to shift towards the origin.

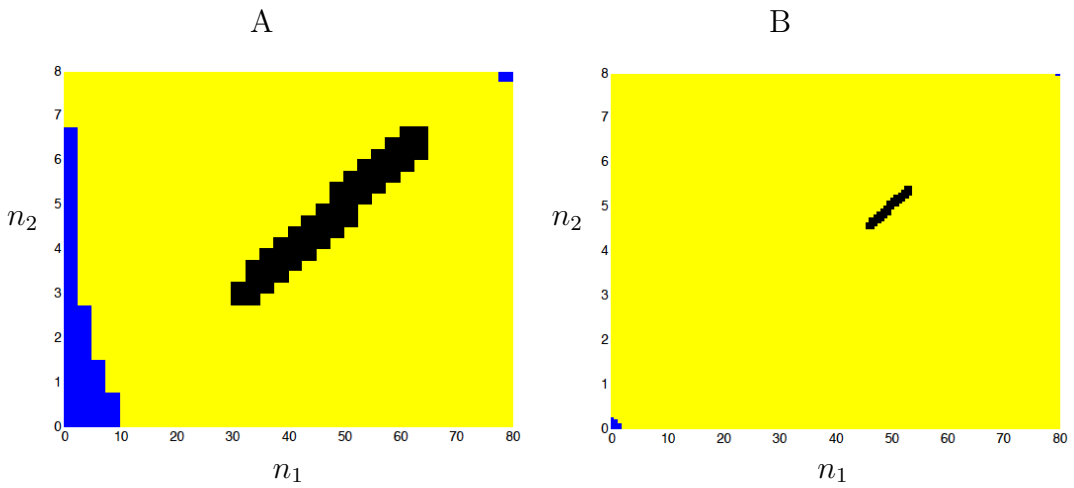

Figure 5.1: Basins of attraction: A at depth 10: B at depth 14

Figure 5.2 shows the basins of attraction for all four cases at a depth of 14.

The basin for Case 2 takes up 99.98% of the root box while the basins for Cases 3 and 4 are 99.24% and 99.35% respectively.

The basins around the non-trivial equilibrium for each case vary in shape and size, but follow the same basic form. We have not yet considered basins around the trivial equilibrium. Although the trivial equilibrium is unstable, it's isolating neighborhood will have a basin of attraction. However, since trajectories can exit from the isolating neighborhood, we can easily see how a trajectory could move into the isolating neighborhood for the trivial equilibrium and then up towards the non-trivial equilibrium.

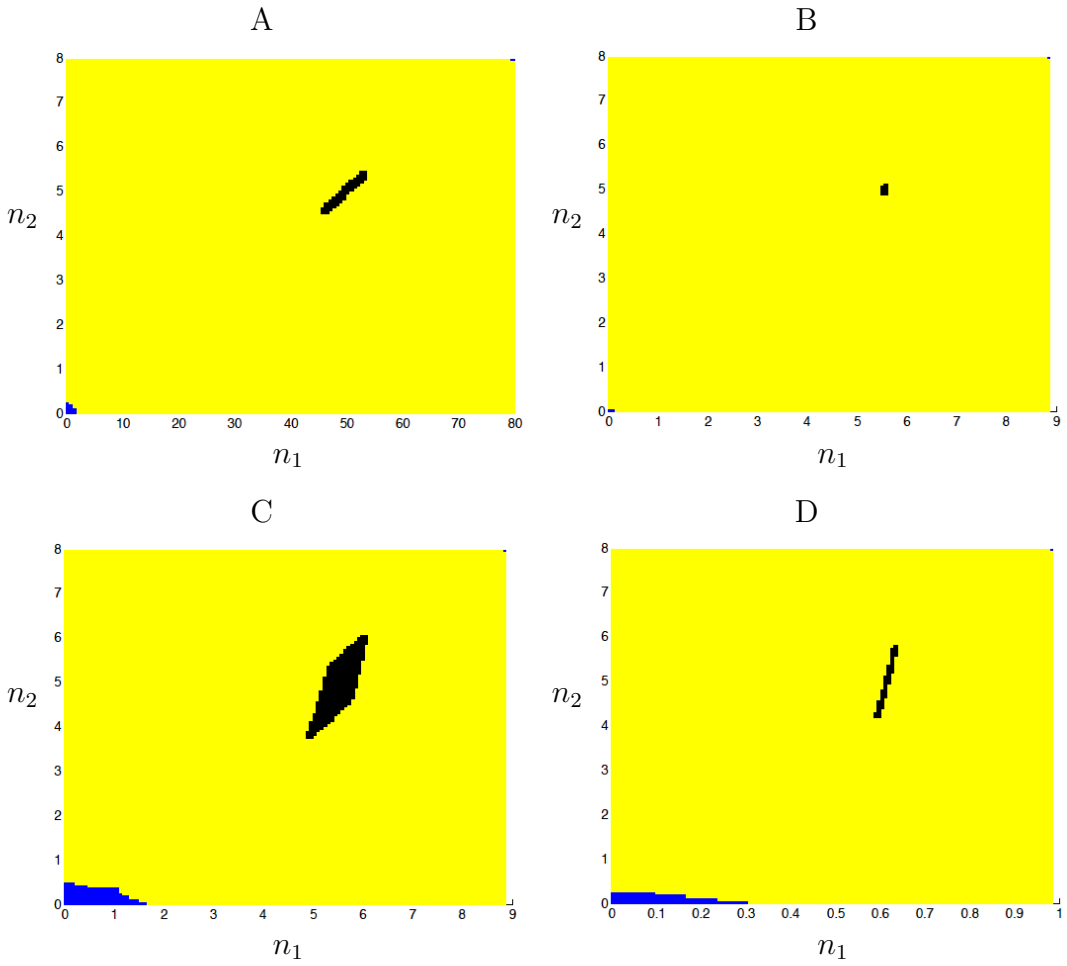

Figure 5.2: Basins of attraction: Trajectories with initial conditions in the basin enter the isolated neighborhood after a finite number of steps and never leave.

Chapter 6

Conclusions and Implications

The main goal of this paper is to study basins of attraction in order to build a better understanding of global system dynamics. More specifically, we aim to develop techniques that might be used to better conservation efforts by making them more efficient. With better information of system dynamics populations can be managed by controlling species into a particular basin instead of moving them all the way to the equilibrium.

When faced with a growing invasive species, eradicating the species can be difficult and practically impossible. Knowing the basins of attraction, conservationists would only have to push the population numbers into the desired basin and let them limit to a neighborhood of the desired equilibrium.

In this study, we focus on the dynamics of one population with two stages limited in growth by density dependent fertility. We analyze the system in three different ways 1) linearization around each equilibrium, 2) computing the Conley Index of isolated invariant sets, and 3) computing basins of attraction for neighborhoods containing attracting equilibria. All three methods return corroborating results starting with the very local information from the linearization procedure and working through the global results brought forward by the computation of basins.

The basins of attraction in the two-dimensional model cover the majority of the studied regions. As modeled, these species exhibit incredibly high resilience, by that we mean they have a strong ability to recover from disturbance. These models also show us that species with these life history parameters would be very hard to control from a management perspective. Human intervention would have to push the populations all the way to extinction in order to eradicate them. Without biological controls, these species will be fast to establish themselves and difficult to remove.

Other biological controls often exist in nature making it more difficult for in-

vasive species to establish a stable population. When population density is low, the Allee effect, a commonly known phenomenon in conservation biology, predicts that population and reproductive uncertainty will limit the species' initial growth if not drive it to extinction. For instance, small populations may not have the correct gender ratio or high enough interaction between individuals to promote reproduction [14]. This principle impacts the density dependent fertility term in this model. Where we predict that the fertility rate will increase with smaller populations all the way to extinction, the Allee effect shows that there will come a point where small population size will inhibit reproduction.

Appropriate modifications of the model may also be studied using the techniques presented here. In particular, even if the resulting model proves too unwieldy for traditional linearization techniques, the Conley Index can still be used to check for fixed points in isolated invariant sets and the algorithm to compute basins is still applicable. These techniques are immediately applicable to to more complicated models, just as they are to the model illustrated here.

As stated in the introduction, the study was motivated by a two species model reflecting invasive species dynamics. Table 4.3 gives some of the information from the linearization of the two species model, but the full analysis using the Conley Index and computing basin is not included in this paper. The immediate goal is to extend the understanding of the four-dimensional model to a comparable level to the two-dimensional model, namely by computing the Conley Index for each of the equilibria and the basins of attraction for the neighborhood of the attracting coexistence equilibrium found in the linearization.

The techniques applied to the two-dimensional model are directly applicable to the four-dimensional model. However, using the same division algorithm is problematic. Dividing a four-dimensional box into significantly small pieces takes many more subdivisions since each step only divides in one coordinate direction. To solve this problem, we plan to create an adaptive subdivision algorithm. This algorithm creates the basin of attraction after some reasonable number of subdivisions and then only subdivide further the area that is not covered by the basin. This approach will allow the edges of the basin to be refined and expanded without unnecessarily dividing and storing the boxes that are clearly in the basin.

The two-dimensional system shows how some populations will behave when introduced to a new, friendly environment. We see how the species would react to being transplanted into an area with no competition. The four-dimensional system is more useful because it starts to consider species interaction with competition for resources. Knowledge of the basins of attraction when ecosystem dynamics are considered would allow conservationists to use resources more effectively to move a system into the correct basin and let it limit naturally into a neighborhood of

the desired equilibrium rather than trying to move the system all the way to the desired equilibrium through environmentally disruptive methods. The focus on global dynamics is what makes this a useful and powerful approach to analyzing population models.

Bibliography

[1] Computational Homology Project (CHomP). (http://chomp.rutgers.edu/projects/).

[2] Jorge A. Ahumada, Dennis Lapointe, and Michael D. Samuel. Modeling the population dynamics of *Culex quinquefasciatus* (diptera: Culicidae), along an elevation gradient in Hawaii. *Journal of Medical Entomology*, 41(6):1157–1170, 2004.

[3] Kathleen T. Alligood, Tim D. Sauer, and James A. Yorke. *Chaos: An Introduction to Dynamical Systems*. Springer, New York, 1996.

[4] Joseph Briggs, Kathryn Dabbs, Michael Holm, Joan Lubben, Richard Rebarber, Brigitte Tenhumberg, and Daniel Riser-Espinoza. Structured population dynamics: An introduction to integral modeling. *Mathematics Magazine*, 83(4):243–257, October 2010.

[5] Hal Caswell. *Matrix Population Models*. Sinauer Associates, Inc., Sunderland, MA, 2nd edition, 2001.

[6] Larry B. Crowder, Deborah T. Crouse, Selina S. Heppell, and Thomas H. Martin. Predicting the impact of turtle excluder devices on loggerhead sea turtle populations. *Ecological Applications*, 4(3):437–445, Aug 1994.

[7] Sarah Day, Rafael Frongillo, and Rodrigo Tevi no. Algorithms for rigorous entropy bounds and symbolic dynamics. *SIAM Journal of Applied Dynamical Systems*, 7(4):1477–1506, 2008.

[8] Michael Dellnitz, Gary Froyland, and Oliver Junge. The algorithms behind GAIO - set oriented numerical methods for dynamical systems. In *Ergodic Theory, Analysis, and Efficient Simulation of Dynamical Systems*. Springer, Berlin, 2001.

[9] Bo Ebenman. Dynamics of age- and size-structured populations: Intraspecific competition. In Bo Ebenman and Lennart Persson, editors, *Size-Structured Populations: Ecology and Evolution*. Springer-Verlag, 1988.

[10] Leonard A. Freed, Rebecca L. Cann, M. Lee Goff, Wendy A. Kuntz, and Gustav R. Bodner. Increase in avian malaria at upper elevation in Hawai'i. *The Condor*, 107:753–764, 2005.

[11] Masami Fujiwara, Georgia Pfeiffer, May Boggess, Sarah Day, and Jay Walton. Coexistence of stage-structured populations. *preprint*, 2011.

[12] P. H. Leslie. On the use of matrices in certain population mathematics. *Biometrika*, 33(3):183–212, November 1945.

[13] E. G. Lewis. On the generation and growth of a population. *Sankhya: The Indian Journal of Statistics*, 6(1):93–96, 1942.

[14] Péter K. Molnár, Andrew E. Derocher, Mark A. Lewis, and Mitchell K. Taylor. Modelling the mating system of polar bears: a mechanistic approach to the allee effect. *Proceedings of the Royal Society*, 275:217–226, 2007.

[15] Michael G. Neubert and Hal Caswell. Density-dependent vital rates and their population dynamic consequences. *Mathematical Biology*, 41:103–121, 2000.

[16] Elgin Perry, Greg Seegert, Joe Vondruska, Timothy Lohner, and Randy Lewis. Modeling possible cooling-water intake system impacts on Ohio River fish populations. In Douglas A. Dixon, John A. Veil, and Joe Wisniewski, editors, *Defining and Assessing Adverse Environmental Impact from Power Plant Impingement and Entrinment of Aquatic Organisms*. A.A. Balkema Publishers, 2003.

[17] Zulima Tablado, José L. Tella, José A. Sánchez-Zapata, and Fernando Hiraldo. The paradox or the long-term positive effects of a North American crayfish on a European community of predators. *Conservation Biology*, 24(5):1230–1238, October 2010.

[18] J. Gaston Zamora-Abrego, Yuan-Mou Chang, J. Jaime Zuniga-Vega, Adrian Nieto-Montes de Oca, and Jerald B. Johnson. Demography of a knob-scaled lizard in northeastern Queretaro, Mexico. *Herpetologica*, 66(1):39–51, 2010.